

# ChemComm

Accepted Manuscript



This is an *Accepted Manuscript*, which has been through the Royal Society of Chemistry peer review process and has been accepted for publication.

*Accepted Manuscripts* are published online shortly after acceptance, before technical editing, formatting and proof reading. Using this free service, authors can make their results available to the community, in citable form, before we publish the edited article. We will replace this *Accepted Manuscript* with the edited and formatted *Advance Article* as soon as it is available.

You can find more information about *Accepted Manuscripts* in the [Information for Authors](#).

Please note that technical editing may introduce minor changes to the text and/or graphics, which may alter content. The journal's standard [Terms & Conditions](#) and the [Ethical guidelines](#) still apply. In no event shall the Royal Society of Chemistry be held responsible for any errors or omissions in this *Accepted Manuscript* or any consequences arising from the use of any information it contains.

## COMMUNICATION

# LiFSI-LiTFSI binary-salt electrolyte to achieve high capacity and cycle stability for Li-S battery

Cite this: DOI: 10.1039/x0xx00000x

J. J. Hu, G. K. Long, S. Liu, G. R. Li and X. P. Gao \*

Received 00th January 2012,

Accepted 00th January 2012

DOI: 10.1039/x0xx00000x

www.rsc.org/

**LiFSI and LiTFSI are combined to form a binary-salt electrolyte with higher ionic conductivity and lower viscosity for Li-S battery. A high capacity and stable cycle performance of the sulfur-based composite with high sulfur content are realized in the electrolyte, accompanied simultaneously with the homogeneous lithium deposition on anode.**

Sulfur, with a theoretical capacity of  $1675 \text{ mAh}\cdot\text{g}^{-1}$ , is considered as a promising alternative cathode material for high energy density battery system.<sup>1</sup> However, some intrinsic properties, such as the low ionic and electronic conductivity of sulfur and lithium sulfide, the “shuttle phenomenon” of the dissolved intermediate polysulfides, and the volume expansion caused by electrochemical dissolution-deposition reaction, lead to poor cycle stability of sulfur cathodes.<sup>2</sup> In recent years, the electrochemical performance of the sulfur cathodes has been improved greatly by encapsulating or immobilizing sulfur into various conductive materials by physical barrier,<sup>3</sup> capillarity,<sup>4</sup> chemical bonding,<sup>5</sup> hydrogen bond, and/or other weak interactions<sup>6</sup> in order to restrict the dissolution of polysulfides. However, due to the quasi “liquid” nature of the sulfur cathode,<sup>7</sup> the dissolution of polysulfides is essential to effectively utilize the active material,<sup>8</sup> especially for the cathode with high sulfur loading. In addition, the diffusion of soluble species caused by the inherent electric field and the concentration gradient should be regulated by the electrolyte.<sup>9</sup> Therefore, it is highly significant to explore new electrolyte for fabricating high energy Li-S battery with desirable performance.

Recently, the concentrated electrolytes containing lithium bis(trifluoromethanesulfonyl)imide ( $\text{Li}[\text{N}(\text{SO}_2\text{CF}_3)_2]$ , LiTFSI) provide novel approaches to restricting the dissolution of lithium polysulfides from sulfur cathode side and the growth of lithium dendrites from anode side.<sup>10</sup> The common ion effect and the high viscosity of the electrolyte could improve the cycle

stability of the sulfur cathodes. Nevertheless, the high viscosity in the concentrated electrolyte may limit the sulfur utilization and slow down the reaction kinetics at the same time.<sup>11</sup> Novel electrolytes, providing simultaneously high capacity and good cycle stability, are urgently required for sulfur cathode with high sulfur loading.

Lithium bis(fluorosulfonyl) imide ( $\text{Li}[\text{N}(\text{SO}_2\text{F})_2]$ , LiFSI), which has a similar structure and smaller size than LiTFSI, shows satisfactory electrochemical performance owing to higher ionic conductivity in the carbonate based electrolyte.<sup>12</sup> In this communication, LiFSI is introduced into the ether based electrolyte for Li-S battery system, and the synergies between LiFSI and LiTFSI on both the sulfur cathode and the lithium anode are characterized and discussed.

**Table 1** Ionic conductivity ( $\sigma$ ) and viscosity ( $\eta$ ) of LiFSI, LiTFSI and mixed electrolytes at 25 °C.

Concentration	$\sigma / \text{mS}\cdot\text{cm}^{-1}$		$\eta / \text{cP}$	
	LiFSI	LiTFSI	LiFSI	LiTFSI
1 M	11.99	9.67	2.45	2.56
1.5 M	11.80	7.82	2.76	4.68
2 M	11.51	6.19	4.30	6.93
2.5 M	10.98	5.08	6.46	11.04
3 M	9.96	3.56	8.75	16.12
1 M LiFSI + 0.5 M LiTFSI	11.09		3.13	
0.5 M LiFSI + 1 M LiTFSI	10.45		3.90	

The cathode used herein with sulfur loading up to  $1.8 \text{ mg}/\text{cm}^2$  is composing of electropolymerized polymer coating carbon and sulfur in the weight ratio of 1:4 (79.05 wt. % as measured by TG), with good structural integrity and high electronic conductivity. Details of the sulfur-based composite are available in Fig. S1-5. Given that LiFSI outperforms LiTFSI in

ionic conductivity ( $\sigma$ ) and viscosity ( $\eta$ ) in ether based electrolyte (**Table 1**), LiFSI is a potential alternative salt in ether based electrolyte for Li-S battery. The sulfur cathode in the electrolyte with the single LiFSI salt shows a large initial capacity, but poor cycle stability. In addition, the cycle deterioration becomes heavier with increasing the LiFSI concentration, while the stable cycle and low capacity of the sulfur cathode are achieved in the electrolyte with the concentrated LiTFSI (**Fig. S6**). The high initial capacity is mainly related to the higher affinity of LiFSI towards polysulfides and electrode surface based on the calculated charge distribution (**Fig. S7**). Meanwhile, the high ionic conductivity and the low viscosity are also beneficial to reach the high initial capacity of the sulfur cathode in the electrolyte with single LiFSI salt. However, the low viscosity (**Table 1**) promotes the diffusion of polysulfides, resulting in poor cycle life. In particular, the coulombic efficiency of the sulfur cathode is lower in the electrolyte with single LiFSI salt (**Fig. S9**). Moreover, the common ion effect is not acted in concentrated electrolyte due to the low solubility and high reactivity of LiFSI.<sup>13</sup> Therefore, combined with the stronger interaction between LiFSI and polysulfides from the calculated charge distribution, these multi-factors lead to the serious competition between dissolution and disproportionation of polysulfides and the undesired solid-electrolyte interphase (SEI) composition.<sup>14</sup> In order to realize high capacity and long cycle stability, binary-salt electrolytes with different constituents of LiFSI and LiTFSI are measured. Here, the concentration of 1.5 M  $\text{Li}^+$  is chosen for the comprehensive performance of moderate viscosity and ionic conductivity of the electrolyte, large discharge capacity and good cycle stability of the cathode. The series of the electrolytes evaluated are 1.5 M LiFSI, 1 M LiFSI+0.5 M LiTFSI, 0.5 M LiFSI+1 M LiTFSI and 1.5 M LiTFSI in 1,3-dioxolane (DOL) and 1,2-dimethoxyethane (DME) (1:1 by volume), respectively.

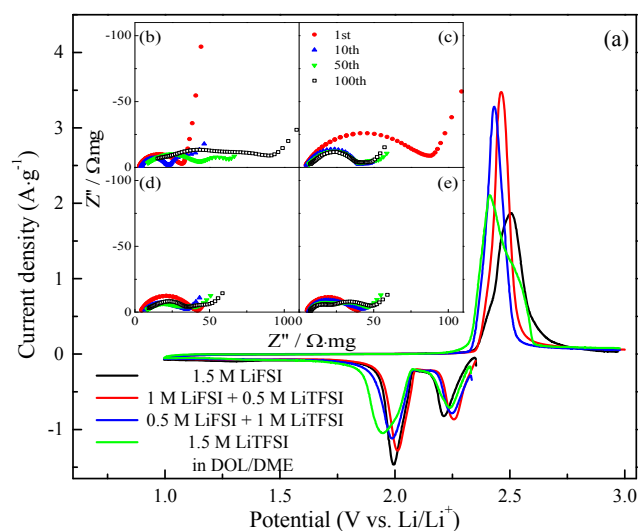


**Fig. 1.** (a) Initial cyclic voltammograms of the sulfur cathode in different electrolytes in the potential range of 1.0–3.0 V at a scan rate of 0.1  $\text{mV}\cdot\text{s}^{-1}$ . Nyquist plots of the cells after different cycles at a current

density of 200  $\text{mA}\cdot\text{g}^{-1}$  in the DOL/DME (1:1, by volume) electrolytes with 1.5 M LiFSI (b), 1 M LiFSI + 0.5 M LiTFSI (c), 0.5 M LiFSI + 1 M LiTFSI (d), and 1.5 M LiTFSI (e).

The initial cyclic voltammograms (CVs) of the sulfur cathode in different electrolytes are compared in **Fig. 1a**. When LiFSI salt is introduced into the electrolyte, the profiles of two cathodic peaks and one anodic peak are almost identical to those in the electrolyte with LiTFSI salt. In the cathodic process, the reduction peak at higher potential is attributed to the formation of long chain lithium polysulfides ( $\text{Li}_2\text{S}_x$ ,  $4 \leq x \leq 8$ ), and the peak in the lower potential region is related to the further reduction of polysulfides to insoluble  $\text{Li}_2\text{S}_2$  and  $\text{Li}_2\text{S}$ . In the anodic process, the peak around 2.5 V (vs  $\text{Li}/\text{Li}^+$ ) can be ascribed to the oxidation of insoluble products to  $\text{Li}_2\text{S}_8$  and/or even further to sulfur.<sup>11</sup> With increasing LiFSI proportion in the binary-salt electrolyte, the two reduction peaks shift to higher potential, and the anodic peak becomes sharper, indicating the improved reversibility and sulfur utilization. In particular, the binary-salt electrolyte is superior to the LiTFSI-based electrolyte due to the relatively high ion conductivity and low viscosity, contributing to the low polarization and high utilization of active sulfur.

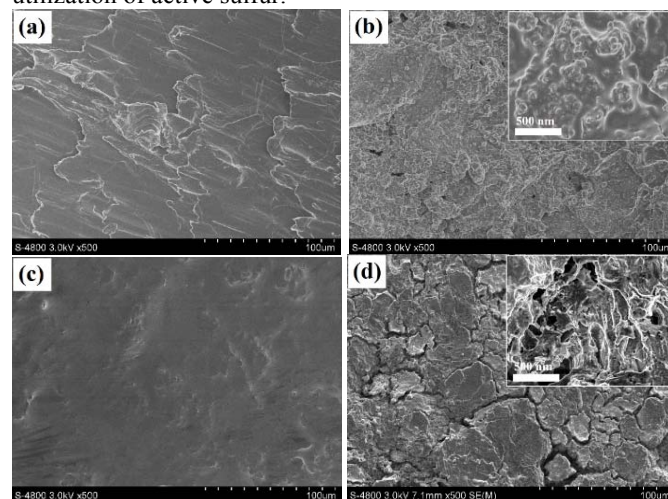


**Fig. 2.** SEM images of the metallic lithium anodes. (a) fresh anode, and cycled anodes after 100 cycles in (b) 1.5 M LiFSI electrolyte, (c) 1 M LiFSI + 0.5 M LiTFSI electrolyte, and (d) 1.5 M LiTFSI electrolyte.

Additionally, the better reversibility and stability are confirmed by electrochemical impedance spectroscopy (EIS) and scanning electron microscopy (SEM). The cycle performance of Li-S battery is highly related to the interface stability due to the nature of the dissolution-deposition reaction of both electrodes. Both a serious aggregation of insulated  $\text{Li}_2\text{S}_2/\text{Li}_2\text{S}$  on the cathode surface and a rough surface of lithium metal are detrimental to the cell cycle life.<sup>14-15</sup> In Li/S cell, the electrochemical reaction process is mainly determined by the sulfur cathode with insulated S and  $\text{Li}_2\text{S}_2/\text{Li}_2\text{S}$  on the surface. Therefore, the information from metallic lithium anode side in EIS is almost negligible, and the kinetic reaction of sulfur cathode is dominant in EIS. As shown in **Fig. 1b-e**, Nyquist plots consist of two semicircles in the high frequency

region and a straight line in the low frequency region. The semicircle in the lower frequency region is ascribed to the surface charge transfer process of the electrodes, influenced by the formation of the SEI and the insulating layer of  $\text{Li}_2\text{S}_2/\text{Li}_2\text{S}$ . Contrary to the obviously increasing surface charge-transfer resistance and Warburg diffusion impedance in the electrolyte with individual 1.5 M LiFSI and 1.5 M LiTFSI, the electrochemical parameters are much smaller in 1M LiFSI+0.5M LiTFSI binary-salt electrolyte after 100 cycles (Table S1). Meanwhile, the sulfur cathode after 100 cycles in the electrolyte with 1 M LiFSI + 0.5 M LiTFSI shows the best surface integrity (Fig. S8). In particular, the obvious variation in the surface morphology of the metallic lithium anodes after 100 cycles in the different electrolytes is presented in Fig. 2. In the electrolyte with 1.5 M LiTFSI, the surface crack and the pulverization of lithium anode are serious after 100 cycles, which could result in sharp drop of the Li-S cell performance.<sup>16</sup> In the electrolyte with 1.5 M LiFSI, a rough surface with protuberances forms due to the fast lithium deposition, which is the origin of lithium dendrites. On the contrary, a smooth surface of lithium anode without the dendrite formation can be clearly observed in the LiFSI-LiTFSI binary-salt electrolyte after 100 cycles, which has become more uniform during repeated charge/discharge processes as compared with the fresh lithium anode. The comparable surface characteristic of the lithium anode was also reported,<sup>13</sup> in which the dendrite-free metallic lithium after cycling was observed in the Li/Li symmetric cell in a LiFSI-LiTFSI/DOL-DME electrolyte system. Besides, the highly reversible deposition-stripping of lithium could occur at graphite electrodes by adding LiTFSI to the [FSI]<sup>-</sup> based ionic liquids.<sup>17</sup> Therefore, the synergy of the two salts brings more homogeneous and integrated interfaces on both electrodes, improving the cycle stability of Li-S battery.

The initial charge-discharge profiles of the sulfur cathode measured by the galvanostatic method are shown in Fig. 3a. There are two potential plateaus around 2.3 and 2.0 V (vs  $\text{Li}/\text{Li}^+$ ) in the discharge process, corresponding to the formation of high order and low order lithium polysulfides, respectively. For the profiles among various electrolytes, the notable difference is that the low potential plateau of sulfur cathode extends with increasing the LiFSI proportion in the electrolyte, leading to the increase of the discharge capacity. Specifically, the maximum discharge capacities of the sulfur-based composites are 1075 and 1052  $\text{mAh g}^{-1}\text{-composite}$  in the electrolyte with 1.5 M LiFSI and 1 M LiFSI+0.5 M LiTFSI, respectively, corresponding to 1359.9 and 1330.8  $\text{mAh g}^{-1}\text{-sulfur}$ . It implies that the high utilization of active sulfur in the composite with high sulfur loading can be obtained by introducing LiFSI into the electrolyte, in accordance with the CV results. After 20 cycles, the potential difference between the charge and discharge plateaus becomes larger due to the accumulation of passivation layer on electrodes and the increasing viscosity of the electrolyte caused by the dissolution of polysulfides. Whereas, the synergy of the two salts in the electrolyte brings lower polarization and high discharge capacity.

Fig. 3c compares the cycle performance of the sulfur cathode in different electrolytes. Contrary to the trend in initial capacity, the good cycle stability is obtained by increasing the LiTFSI proportion in the electrolyte. In the binary-salt electrolyte, good high-rate performance and high coulombic efficiency can be also achieved (Fig. S9-10). The best result from the electrolyte with 1 M LiFSI + 0.5 M LiTFSI is ascribed to the facilitated migration of ions in the electrolyte, better wettability coupled with the lower viscosity, and the lower polarization by the synergy as discussed above. Fig. 3d shows the prolonged cycle life of the sulfur cathode in 1 M LiFSI + 0.5 M LiTFSI at different current densities. The capacity is stable with cycling at high current densities and retains 710, 588, 551 and 405  $\text{mAh g}^{-1}\text{-composite}$  after 100 cycles at 200, 1000, 2000 and 5000  $\text{mA g}^{-1}\text{-composite}$ , respectively.

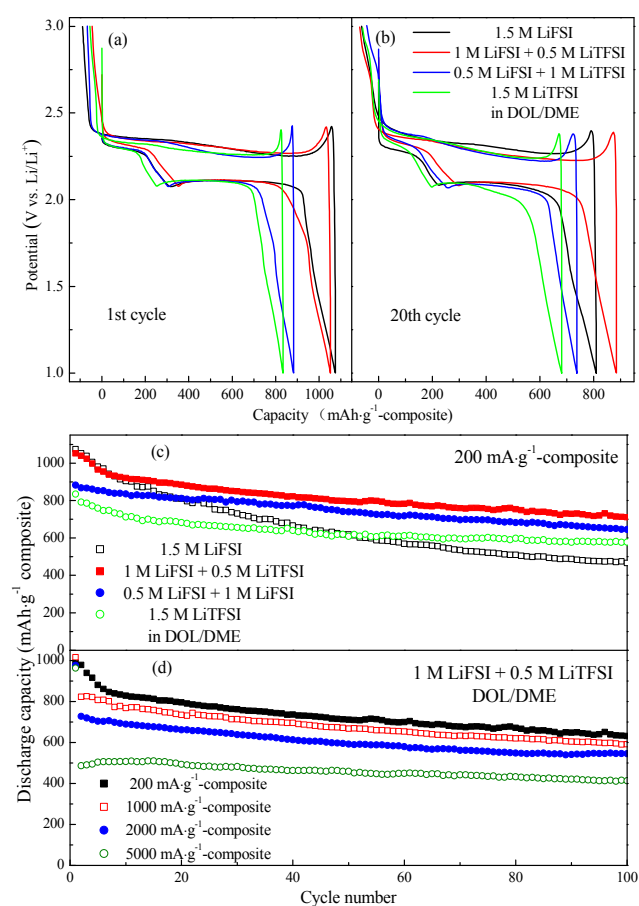


**Fig. 3.** (a) Initial and (b) 20th discharge-charge curves of the sulfur cathode in different electrolytes at the current density of  $200 \text{ mA g}^{-1}\text{-composite}$ . (c) Cycle stability of the sulfur cathode in different electrolytes at the current density of  $200 \text{ mA g}^{-1}\text{-composite}$ . (d) Prolonged cycle performance of the sulfur cathode in the electrolyte with 1 M LiFSI + 0.5 M LiTFSI at different current densities. All the initial discharge current density is  $200 \text{ mA g}^{-1}\text{-composite}$ .

As a dominant component in Li-S battery, the electrolyte not only works as an effective ionic transporter, but also affects the interfacial architecture by molecular interactions based on the dissolution-deposition reaction for both sulfur cathode and



lithium anode. LiFSI, with small anionic size (the radius of [FSI]<sup>-</sup> and [TFSI]<sup>-</sup> is 0.289 nm and 0.329 nm, respectively<sup>18</sup>), is a suitable constituent in the electrolyte to achieve better infiltration and faster ionic transportation. The difference in size and calculated charge distribution (Fig. S7) between [FSI]<sup>-</sup> and [TFSI]<sup>-</sup> may result in the different interaction with the polysulfides and affinity towards the electrode surface. The overlapping of electron cloud and the steric hindrance arisen from each other can offer shielding effect in the electrolyte, which is attributed to the stable electrostatic shield by ion-pairing interactions in multi-anion system, similar to that in multi-cation system.<sup>19</sup> After introducing LiFSI into the electrolyte with LiTFSI, high capacity, stable cycle life and high coulombic efficiency are achieved. Moreover, the synergy between LiFSI and LiTFSI is observed correspondingly, insuring the homogeneous lithium deposition on anode surface in the stable electrostatic shield.

## Conclusions

In summary, the shortages in cycle stability and initial discharge capacity of the sulfur cathode in the electrolyte with individual LiFSI or LiTFSI salts are balanced by combining two salts. The sulfur-based composite with high sulfur content (79.05 wt.%) in the optimized electrolyte with 1 M LiFSI+0.5 M LiTFSI in DOL/DME exhibits high discharge capacity, stable cycle performance and good high-rate capability. The optimization of the electrolyte components and further investigation of the molecular interactions should achieve better performance. The result and discussion provided in this study will contribute to the understanding of sulfur electrochemistry, lithium deposition and the improvement of Li-S battery.

## Acknowledgements

Financial Supports from the 973 Program (2015CB251100), NSFC (21421001), and MOE Innovation Team (IRT13022) of China are gratefully acknowledged.

## Notes and references

<sup>a</sup> Institute of New Energy Material Chemistry, Collaborative Innovation Center of Chemical Science and Engineering (Tianjin), Tianjin Key Laboratory of Metal and Molecule Based Material Chemistry, Nankai University, Tianjin 300071, China. Fax: +86-22-23500876; Tel: +86-22-23500876; E-mail: [xpgao@nankai.edu.cn](mailto:xpgao@nankai.edu.cn)

† Experimental details of synthesis, electrochemical measurements, structure analyses of the sulfur based-composite. The calculated Electronic Static Potential (ESP) and Mulliken atomic charges of [FSI]<sup>-</sup> and [TFSI]<sup>-</sup> by Gaussian. See DOI: 10.1039/c000000x/

- X. L. Ji and L. F. Nazar, *J. Mater. Chem.*, 2010, **20**, 9821; X. P. Gao and H. X. Yang, *Energy Environ. Sci.*, 2010, **3**, 174; D. W. Wang, Q. C. Zeng, G. M. Zhou, L. C. Yin, F. Li, H. M. Cheng, I. R. Gentle and G. Q. Lu, *J. Mater. Chem. A*, 2013, **1**, 9382; H. B. Yao, G. Y. Zheng, P. C. Hsu, D. S. Kong, J. J. Cha, W. Y. Li, Z. W. Seh, M. T. McDowell, K. Yan, Z. Liang, V. K. Narasimhan, and Y. Cui, *Nat. Commun.* 2014, **5**, 3943.
- Y. Yang, G. Y. Zheng and Y. Cui, *Chem. Soc. Rev.*, 2013, **42**, 3018; J. Hu, G. R. Li and X. P. Gao, *J. Inorg. Mater.*, 2013, **28**, 1181.
- G. C. Li, G. R. Li, S. H. Ye and X. P. Gao, *Adv. Energy Mater.*, 2012, **2**, 1238; Y. S. Su and A. Manthiram, *Chem. Comm.*, 2012, **48**, 8817; C. F. Zhang, H. B. Wu, C. Z. Yuan, Z. P. Guo and X. W. Lou, *Angew. Chem. Int. Ed.*, 2012, **51**, 1; G. Q. Ma, Z. Y. Wen, J. Jin, Y. Lu, X. W. Wu, M. F. Wu, and C. H. Chen, *J. Mater. Chem. A*, 2014, **2**, 10350.
- X. L. Ji, K. T. Lee and L. F. Nazar, *Nat. Mater.*, 2009, **8**, 500; J. Kim, D. J. Lee, H. G. Jung, Y. K. Sun, J. Hassoun, and B. Scrosati, *Adv. Funct. Mater.*, 2012, **23**, 1076; G. Y. Zheng, Y. Yang, J. J. Cha, S. S. Hong and Y. Cui, *Nano Lett.*, 2011, **11**, 4462.
- J. L. Wang, J. Yang, J. Y. Xie and N. X. Xu, *Adv. Mater.*, 2002, **14**, 963; J. M. Zheng, J. Tian, D. X. Wu, M. Gu, W. Xu, C. M. Wang, F. Gao, M. H. Engelhard, J. G. Zhang, J. Liu, J. Xiao, *Nano Lett.*, 2014, **14**, 2345.
- J. F. Chen, Q. Zhang, Y. N. Shi, L. L. Qin, Y. Cao, M. S. Zheng and Q. J. Dong, *Phys. Chem. Chem. Phys.*, 2012, **14**, 5376; L. W. Ji, M. M. Rao, H. M. Zheng, L. Zhang, Y. C. Li, W. H. Duan, J. H. Guo, E. J. Cairns, and Y. G. Zhang, *J. Am. Chem. Soc.*, 2011, **113**, 18522.
- R. Demir-Cakan, M. Morcrette, F. Nouar, C. Davoisne, T. Devic, D. Gonbeau, R. Dominko, C. Serre, G. Ferey and J. M. Tarascon, *J. Am. Chem. Soc.*, 2011, **1133**, 16154.
- S. S. Zhang, *J. Power Sources*, 2013, **231**, 153.
- Z. Q. Jin, K. Xie, X. B. Hong and Z. Q. Hu, *J. Power Sources*, 2013, **242**, 478; M. Cuisinier, P. E. Cabelguen, B. D. Adams, A. Garsuch, M. Balasubramanian, and L. F. Nazar, *Energy Environ. Sci.*, 2014, **7**, 2697.
- E. S. Shin, K. Kim, S. H. Oh and W. I. Cho, *Chem. Comm.*, 2013, **49**, 2004; L. M. Suo, Y. S. Hu, H. Li, M. Armand and L. Q. Chen, *Nat. Commun.*, 2013, **4**, 1481; C. X. Zhu, and A. Manthiram, *J. Phys. Chem. Lett.* 2014, **5**, 2522.
- Y. Z. Zhang, S. Liu, G. C. Li, G. R. Li and X. P. Gao, *J. Mater. Chem. A*, 2014, **2**, 4652.
- B. Philippe, R. Dedryvere, M. Gorgoi, H. Rensmo, D. Gonbeau and K. Edstrom, *J. Am. Chem. Soc.*, 2013, **135**, 9829; L. F. Li, S. S. Zhou, H. B. Han, H. Li, J. Nie, M. Armand, Z. B. Zhou and X. J. Huang, *J. Electrochem. Soc.*, 2012, **158**, A74; H. B. Han, S. S. Zhou, D. J. Zhang, S. W. Feng, L. F. Li, K. Liu, W. F. Feng, J. Nie, H. Li, X. J. Huang, M. Armand and Z. B. Zhou, *J. Power Sources*, 2011, **196**, 3623.
- R. R. Miao, J. Yang, X. J. Feng, J. Hao, J. L. Wan and Y. N. Nuli, *J. Power Sources*, 2014, **271**, 291;
- F. Wu, J. Qian, R. R. Chen, J. Lu, L. Li, H. M. Wu, J. Z. Chen, T. Zhao, Y. S. Ye and K. Amine, *ACS Appl. Mater. Interfaces*, doi: 10.1021/am504345s; G. Y. Zheng, S. W. Lee, Z. Liang, H. W. Lee, K. Yan, H. B. Yao, H. T. Wang, W. Y. Li, S. Chu and Y. Cui, *Nat. Nanotech.* 2014, **9**, 618.
- L. X. Yuan, X. P. Qiu, L. Q. Chen and W. T. Zhu, *J. Power Sources*, 2009, **189**, 127; W. G. Wang, X. Wang, L. Y. Tian, Y. L. Wang, and S. H. Ye, *J. Mater. Chem. A*, 2014, **2**, 4316.
- C. Huang, J. Xiao, Y. Y. Shao, J. M. Zheng, W. D. Bennett, D. P. Lu, L. V. Saraf, M. Engelhard, L. W. Ji, J. G. Zhang, X. L. Li, G. L. Graff and J. Liu, *Nat. Commun.* 2014, **5**, 3015.
- K. Hayamizu, S. Tsuzuki, S. Seki, and Y. Umebayashi, *J. Chem. Phys.*, 2011, **135**, 084505.
- M. J. Frisch, et al. Gaussian 03, Revision C.02, Gaussian, Inc., Wallingford CT, 2004.
- F. Ding, W. Xu, G. L. Graff, J. Zhang, M. L. Sushko, X. L. Chen, Y. Y. Shao, M. H. Engelhard, Z. M. Nie, J. Xiao, X. J. Liu, P. V. Sushko, J. Liu and J. G. Zhang, *J. Am. Chem. Soc.* 2013, **135**, 4450; C. X. Zhu, and A. Manthiram, *J. Phys. Chem. Lett.* 2014, **5**, 2522.